Chalcogenide Letters Vol. 13, No. 9, September 2016, p. 397 - 402

INVESTIGATION OF S/Se RATIO ON THE PROPERTIES OF SOLUTION-PROCESSED CZTSSe SOLAR CELL

Y. ZHANG[b], Y. SUN[a,b*]
[a]*Energy and Materials Engineering Centre,, Tianjin Normal University, Tianjin, 300387, P.R. China*
[b]*College of Materials Science and Engineering, Beijing University of Technology, Beijing, 100124, P.R. China*

In this paper, Cu2ZnSnS4 (CZTS) solar cells absorber layers and Cu2ZnSn(SxSe1-x)4 (CZTSSe) with the S/Se ratio varying between 0 and 1 were prepared by an isopropanol-based solution method. The S/Se ratio dependence of photovoltaic properties have been systematically investigated and the performance of the CZTS-based solar cells has been improved by the optimization process. This research would be helpful for the development of cost effective solution- processed CZTSSe thin film solar cells.

(Received July 19, 2016; Accepted September 1, 2016)

Keywords: CZTSSe; Solution-processed; Solar cells; Efficiency.

1. Introduction

Copper zinc tin sulfide (CZTS) with Kesterite structure have attracted increasing attention and have been considered as one of the most potential substitutes material for low-cost thin-film solar cells[1-6] [1,2]. Solution- processed mothed has recently been shown that they can be competitive fabrication approaches, not only in terms of cost, but in terms of efficiency as well, as demonstrated at the early stage of development of kesterite CZTSSe liquid-coating techniques due to its potential low cost, high-throughput manufacturing, and the ease of control film composition and volatile phases[7-10]. Hydrazine-based slurry system currently holds the most successful approach to fabricate CZTS photovoltaic devices[1, 11-13]. However, in the case of hydrazine-based CZTS solar cells, the solvent of precursor solution limited the large-scale production due to its highly toxic. In order to overcome the limitation of hydrazine-processed CZTS solar cells, various solution-based processes were widely developed to fabricate absorber thin films by many researchers, especially alcohol based solution processes[9, 14-18].

Although the highest efficiency of 12.6 % for CZTSSe-based solar cells has been achieved[1], CZTS is expected to have theoretical efficiency of more than 30% according to Shockley-Queisser photon balance calculations[5, 6]. So far, experimental efficiency is quite low compared with the theoretical limit, and thus more systematic study of factors that affect efficiency of device is required, especially of the structure and photoelectrical properties of absorber layers. One of factors that affect the CZTS solar cell performance is the absorber layer's microstructure, since a monolayer of single crystal grains with sizes on the order of the film thickness is required. It is reported that selenium may enhance grain growth. In addition, controlling the band gap in chalcogenide-based solar cells is important in terms of tailoring the properties of the absorber layer to optimize the device efficiency[19].

In this study, we apply the improving efficiency factors to the alcohol-based solution approach for the fabrication of CZTSSe thin film solar cells. S/Se ratio is a key factor that influences the band gap of absorber layer and efficiency of CZTSSe thin film solar cells was discussed.

*Corresponding author: hxxysyx@mail.tjnu.edu.cn

2. Experimental

The CZTS precursor complex solution consisted of $CuCl_2 \cdot 2H_2O$ (0.15 mol/ L), $ZnCl_2$ (0.102 mol/L), $SnCl_2 \cdot 2H_2O$ (0.085 mol/L), and TAA (0.0625 mol/L) dissolved in isopropanol sequentially. When adding $ZnCl_2$ and $SnCl_2 \cdot 2H_2O$ into copper precursor solution with constant stirring, the color of the alcohol solution changed from a deep green to milk-white. After adding the TAA, the color of the precursor solution changed from milk-white to transparent yellow. All CZTS precursor layers were deposited via dip-coating from the as-prepared transparent precursor solution on Mo-coated glass substrates. To build up the precursor layer thickness, the dip-coating process was repeated 10 times following an intermediate heat treatment at 150 ^oC in air for 10 min to evaporate the solvent. A final annealing was conducted in a graphite box at 500 ^oC for 60 min under S vapor, Se vapor, and mixed S/Se vapor for $CZTS_xSe_{1-x}$ film with different S/Se ratios. After the heat treatment, the samples were cooled naturally to room temperature under inert atmosphere.

The $CZTS_xSe_{1-x}$ absorber film was then processed into photovoltaic devices by chemical bath deposition of CdS (50 nm), RF magnetron sputtering of i-ZnO (50 nm), and indium-doped tin oxide (250 nm). A 110-nm-thick MgF_2 antireflection coating was deposited on top of the device by electron beam evaporation. Silver paint was applied to form the top contact.

The kesterite layers were analyzed by X-ray diffraction (XRD) on German Bruker AXS D8 ADVANCE diffractometer (Cu K_α radiation, λ=1.5405 Å). Raman spectra were recorded using the LabRam HR800 instrument, the wavelength of laser excitation for Raman measurements was 488 nm, and the laser power was ~100 mW. The morphologies and microstructures of the films were observed using a Hitach S4800 field emission scanning electron microscope (FE-SEM) equipped with energy dispersive (EDS). UV-Vis spectra were recorded on a Shimadzu UV-3101PC spectrophotometer. Photovoltaic devices were tested on a Karl Suss probe station and an Agilent 4156C parameter analyzer. J-V data and power conversion efficiencies were obtained using a Keithley 2400 General Purpose Sourcemeter and a Xenon Lamp Solar Simulator (Newport) under AM1.5 (1000 W/m^2) global illumination at 25 ^oC.

3. Results and discussion

Four $CZTS_xSe_{1-x}$ thin film samples with different S/Se ratios have been obtained as shown in Table 1. When sulfurized the CZTS precursor thin film under pure S vapor, pure CZTS thin film was synthesized as measured by EDS (here x=1), while selenized the precursor thin film under pure Se vapor, pure CZTSe thin film was obtained, and the other two thin film samples $CZTS_xSe_{1-x}$ with x=0.4 and 0.7 could be obtained by calcination treatment under mixed S/Se vapors with different amount of S and Se powders in a graphite box.

Table 1 Composition analysis and composition ratios of the samples annealed at 500 ^oC with different S/Se ratios measured by EDS.

Samples	Elemental composition (at %)					Composition ratio	
	Cu	Zn	Sn	Se	S	Cu/(Zn+Sn)	S/(S+Se)
CZTS, x=1	19.80	13.24	10.34	0	56.62	0.84	1
$CZTS_xSe_{1-x}$,x=0.7	20.46	13.28	11.37	17.54	37.34	0.83	0.7
$CZTS_xSe_{1-x}$,x=0.4	20.59	13.20	11.32	32.93	21.96	0.84	0.4
CZTSe, x=0	21.05	13.53	11.23	54.19	0	0.85	0

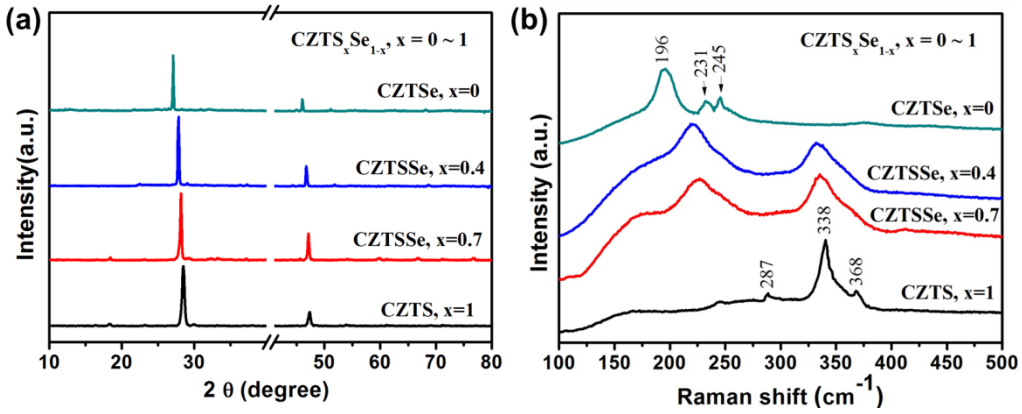

Fig. 1 (a) XRD patterns and (b) Raman spectra of $CZTS_xSe_{1-x}$ samples with different S/Se ratios.

The XRD and Raman analysis could confirm the structure of four different $CZTS_xSe_{1-x}$ thin film samples as shown in Fig. 1. The Fig. 1a shows that the CZTS sample with x=1 obtained from the precursor thin film after annealing under S vapor shows two major diffraction peaks at 28.5 and 47.3º, which can be indexed to the (112) and (220) of kesterite structure Cu_2ZnSnS_4 (JCPDS 26-0575), respectively. The backgrounds of Mo substrate have been deducted since the intensity of Mo substrate is too high to be presented in a limited space. These two main diffraction peaks of the sample $CZTS_xSe_{1-x}$ with x=0.4 and 0.7 move toward lower 2θ angles, which is attributed to the increased lattice spacing of the larger Se atoms partially substituted for smaller S atoms during calcination under mixed S/Se vapors. The main diffraction peaks (2θ=27.2 and 45.0º) of the sample with x=0 after annealing under pure Se vapor correspond to the (112) and (204) of kesterite $Cu_2ZnSnSe_4$ (JCPDS 52-0868). Fig. 1b shows the Raman spectra for obtained four different $CZTS_xSe_{1-x}$ thin films. The sulfurized sample (here x=1) shows a major peak at 338 cm^{-1} and two weak peaks at 287 and 368 cm^{-1}, which are attributed to the CZTS representative mode[20, 21]. Two main peaks between 196 and 338 cm^{-1} can be associated with a CZTSSe phase, and peaks move slightly toward left with the increase of Se content in $CZTS_xSe_{1-x}$ thin films. The selenized sample (x=0) shows the characteristic CZTSe mode at 196, 231 and 245 cm^{-1}. The XRD and Raman analysis indicate the structure of $CZTS_xSe_{1-x}$ samples with different S/Se ratios.

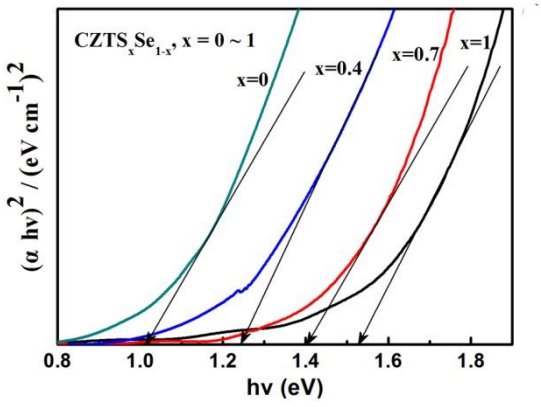

Fig. 2 Band gap determination plot of $CZTS_xSe_{1-x}$ samples

The E_g value of CZTSSe sample can be obtained by extrapolating the linear $(\alpha hv)^2$ versus hv plots to the horizontal axis (α = absorbance, h = Planck's constant, and v = frequency) since CZTS and CZTSe are all direct band gap semiconductors. These E_g values of CZTSSe samples

with different S/Se ratios are shown in Fig. 2. From the extrapolated linear portion, it is obvious that these determined E_g values of four different $CZTS_xSe_{1-x}$ samples (x=1, 0.7, 0.4 and 0) are about 1.53, 1.41, 1.24, and 1.03 eV, respectively. It is found that the band gap value of $CZTS_xSe_{1-x}$ thin film increases monotonically with the increase in the sulfur content. Furthermore, these results show that the relationship between the band gap and the S content can be described by the equation number (1) [22]:

$$E_g(CZTSSe) = (1-x)\, E_g(CZTSe) + x\, E_g(CZTS) + b\, x\, (1-x) \qquad (1)$$

According to the above data, E_g(CZTS) is 1.53 eV (x=1), E_g(CZTSe) is 1.03 eV (x=0), E_g(CZTSSe)=1.41 eV (x=0.7), then we can calculate the bowing parameter b to be approximately 0.142 eV. Hence the relationship between band gap and S content can be described as $E_g(x) = -0.142\, x^2 + 0.642\, x + 1.03$. The calculated band gap of our CZTSSe absorber using x=0.4 is 1.26 eV, which is very close to the band gap value (1.24 eV) estimated by considering the intersecting point from extrapolating the linear region of the plot of $(\alpha h\nu)^2$ vs $h\nu$ to the horizontal axis. Hence, those results indicate that the E_g of CZTSSe thin films derived from solution method following annealing treatment can be controlled almost linearly by varying the S/Se ratio.

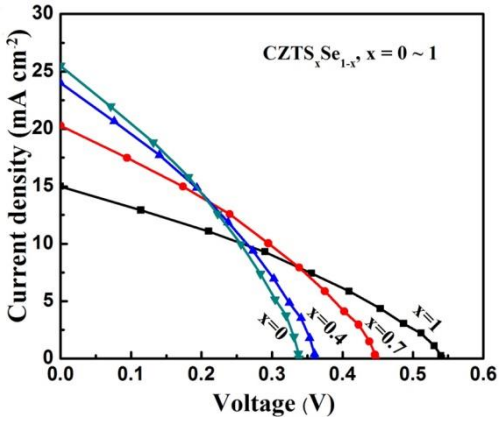

Fig.3 J-V curves of the obtained solar cells with different S/Se ratios.

Subsequently the current density-voltage (J-V) curves of these $CZTS_xSe_{1-x}$-based solar cells with different S/Se ratio are presented in Fig. 3. The four device characteristics are shown in Table 2. With the larger Se content in $CZTS_xSe_{1-x}$ thin film, the V_{oc} value gradually reduced as well the J_{sc} increased, which is consistent with the fact that when E_g becomes larger, then the V_{oc} values increase and J_{sc} reduce accordingly. Comparing these four $CZTS_xSe_{1-x}$-based solar cells, it is found that CZTS based solar cell with biggest band gap value (1.53 eV) presents smaller J_{sc}, while CZTSe based solar cell with smallest band gap value (1.03 eV) shows smaller $V_{oc,}$ and the better efficiency of 3.26 % could be obtained in $CZTS_xSe_{1-x}$-based solar cell with x=0.7. It is worthwhile to observe that the efficiency of CZTSSe solar cell could be greatly improved through suitably tuning the band gap of absorber layers.

Table 2 Characteristics of the solar cells with different S/Se ratios

Cell	V_{oc} / mV	J_{sc} / mA·cm^{-2}	FF / %	Eff. / %
CZTS, x=1	541	15.1	32.3	2.64
$CZTS_xSe_{1-x}$,x=0.7	447	20.3	35.9	3.26
$CZTS_xSe_{1-x}$,x=0.4	360	24.1	34.4	2.98
CZTSe, x=0	340	25.1	31.0	2.65

4. Conclusions

We have fabricated CZTS thin film solar cells through an environmentally alcohol-based solution process. By changing the S/Se ratios in $CZTS_xSe_{1-x}$ thin films, we can tune the band gaps of absorber layer in the range of 1.03-1.53 eV, and better efficiency of CZTSSe solar cell could be obtained through suitably tuning the band gap of absorber layers. The performance of the CZTS-based solar cells has been greatly improved by the optimization process by tuning S/Se ratio in absorber layer. This research would be helpful for the development of cost effective solution-processed CZTSSe thin film solar cells.

Acknowledgements

This work is supported by the Natural Science Foundation of China (No. 21403155), the Tianjin Natural Science Foundation (15JCYBJC17600), and the Beijing Postdoctoral Research Foundation.

References

[1] W. Wang, M.T. Winkler, O. Gunawan, T. Gokmen, T.K. Todorov, Y. Zhu, D.B. Mitzi, Advanced Energy Materials, 4 (2014).
[2] C.M. Fella, Y.E. Romanyuk, A.N. Tiwari, Sol. Energy Mater. Sol. Cells, (2013).
[3] P.M.P. Salomé, H. Rodriguez-Alvarez, S. Sadewasser, Sol. Energy Mater. Sol. Cells, **143,** 9 (2015).
[4] S. Siebentritt, S. Schorr, Progress in Photovoltaics: Research and Applications, **205**, 12 (2012).
[5] M.P. Suryawanshi, G.L. Agawane, S.M. Bhosale, S.W. Shin, P.S. Patil, J.H. Kim, A.V. Moholkar, Materials Technology: Advanced Performance Materials, **28**, 98 (2013).
[6] A. Polizzotti, I.L. Repins, R. Noufi, S.-H. Wei, D.B. Mitzi, Energy & Environmental Science, (2013).
[7] T.K. Chaudhuri, D. Tiwari, Sol. Energy Mater. Sol. Cells, **101,** 46 (2012).
[8] G.M. Ilari, C.M. Fella, C. Ziegler, A.R. Uhl, Y.E. Romanyuk, A.N. Tiwari, Sol. Energy Mater. Sol. Cells, **104**, 125 (2012).
[9] D.B. Mitzi, O. Gunawan, T.K. Todorov, K. Wang, S. Guha, Sol. Energy Mater. Sol. Cells, **95**, 1421 (2011).
[10] Y.E. Romanyuk, C.M. Fella, A.R. Uhl, M. Werner, A.N. Tiwari, T. Schnabel, E. Ahlswede, Sol. Energy Mater. Sol. Cells, **119**, 181 (2013).
[11] O. Gunawan, T.K. Todorov, D.B. Mitzi, Appl. Phys. Lett., **97,** 233506 (2010).

[12] Y. Sun, Y. Zhang, H. Wang, M. Xie, K. Zong, H. Zheng, Y. Shu, J. Liu, H. Yan, M. Zhu, W. Lau, Journal of Materials Chemistry A, **1** , 6880 (2013).
[13] D.A.R. Barkhouse, O. Gunawan, T. Gokmen, T.K. Todorov, D.B. Mitzi, Progress in Photovoltaics: Research and Applications, **20,** 6 (2012).
[14] H. Zhou, C.-J. Hsu, W.-C. Hsu, H.-S. Duan, C.-H. Chung, W. Yang, Y. Yang, Advanced Energy Materials, **3**, 328 (2013).
[15] W. Yang, H.-S. Duan, B. Bob, H. Zhou, B. Lei, C.-H. Chung, S.-H. Li, W.W. Hou, Y. Yang, Adv. Mater., **24,** 6323 (2012).
[16] H. Zhou, T.B. Song, W.C. Hsu, S. Luo, S. Ye, H.S. Duan, C.J. Hsu, W. Yang, Y. Yang, J. Am. Chem. Soc., **135**, 15998 (2013).
[17] J. Zhou, L. You, S. Li, Y. Yang, Mater. Lett., **81,** 248 (2012).
[18] S.-N. Park, S.-J. Sung, D.-H. Son, D.-H. Kim, M. Gansukh, H. Cheong, J.-K. Kang, RSC Advances, **4**, 9118 (2014).
[19] S. Bag, O. Gunawan, T. Gokmen, Y. Zhu, T.K. Todorov, D.B. Mitzi, Energy & Environmental Science, **5,** 7060 (2012).
[20] P.A. Fernandes, P.M.P. Salomé, A.F. da Cunha, J. Alloys Compd., **509**, 7600 (2011).
[21] P.A. Fernandes, P.M.P. Salomé, A.F. da Cunha, Thin Solid Films, **517**, 2519 (2009).
[22] S. Chen, A. Walsh, J.-H. Yang, X.G. Gong, L. Sun, P.-X. Yang, J.-H. Chu, S.-H. Wei, Physical Review B, **83** (2011).